Neuron, Volume *103*

Supplemental Information

Strengthened Temporal Coordination within Pre-existing Sequential Cell Assemblies Supports Trajectory Replay

Usman Farooq, Jeremie Sibille, Kefei Liu, and George Dragoi

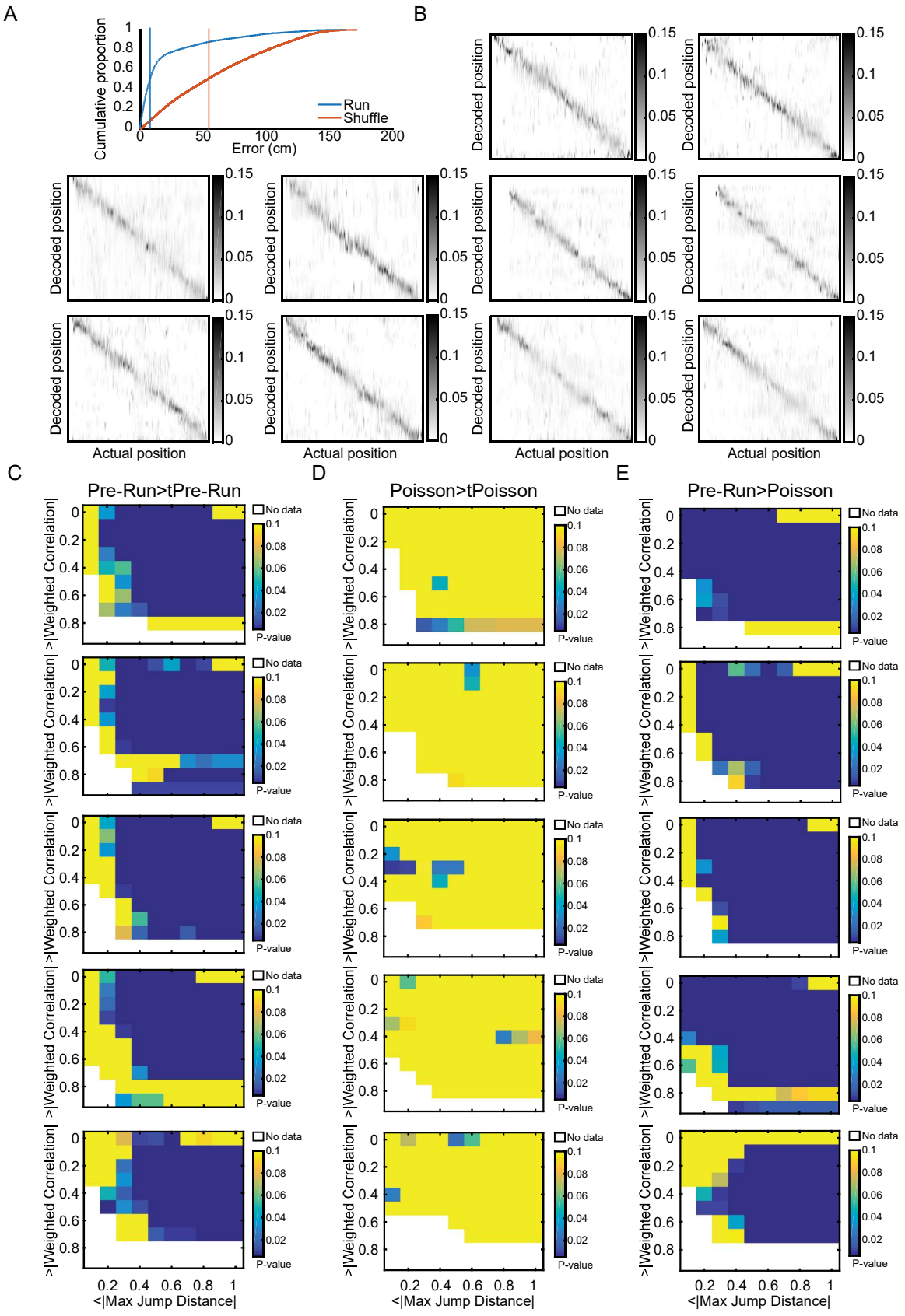

Figure S1. Related to Figure 1. Decoding of animal location during a de novo Run session and Pre-Run sleep at the individual animal level.

(A) Error in decoded location during Run. The median error in decoded location was 7.6 cm, and that of shuffled datasets was 54.3 cm ($P<10^{-10}$, Wilcoxon's ranksum test). Vertical lines represent medians of corresponding distributions.

(B) Confusion matrices for each Run direction in individual animals (n=5 animals).

(C-E) P-value matrices for individual animals, comparisons of: Pre-Run sleep with its time bin shuffle (C), firing rate-matched Poisson with its time bin shuffle (D), and Pre-Run sleep with its five-hundred Poisson surrogate datasets (E).

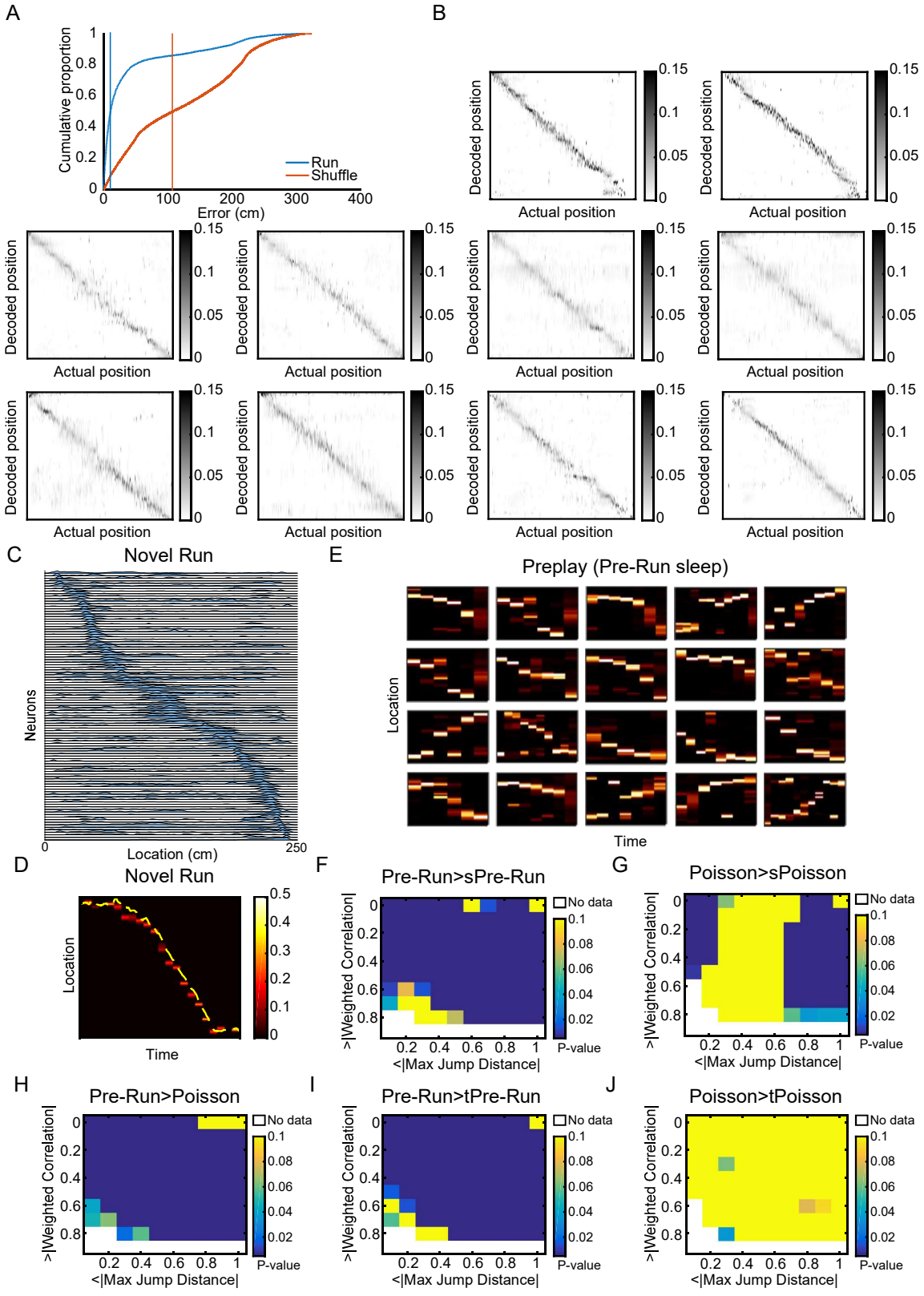

Figure S2. Related to Figure 1. Cross-validation of robustness of preplay in an independent dataset (Grosmark and Buzsaki, 2016). Compressed sequences (preplay) precede spatial experience.
(A) Error in decoding during Run (data versus shuffle: Wilcoxon's ranksum test, $P<10^{-10}$). Vertical lines represent medians of corresponding distributions.
(B) Confusion matrices for Run (n=4 animals).
(C) Place cells during the Run session on a novel track in a novel room.
(D) Decoding of animal trajectory during Run in a single lap.
(E) Examples of preplay sequences in Pre-Run sleep.
(F-J) P-value matrices for individual animals, comparisons of: Pre-Run sleep with its space bin shuffle (F), firing-rate matched Poisson with its space bin shuffle (G), Pre-Run with its five-hundred Poisson surrogate datasets (H), Pre-Run sleep with its time bin shuffle (I) and firing-rate matched Poisson with its time bin shuffle (J).

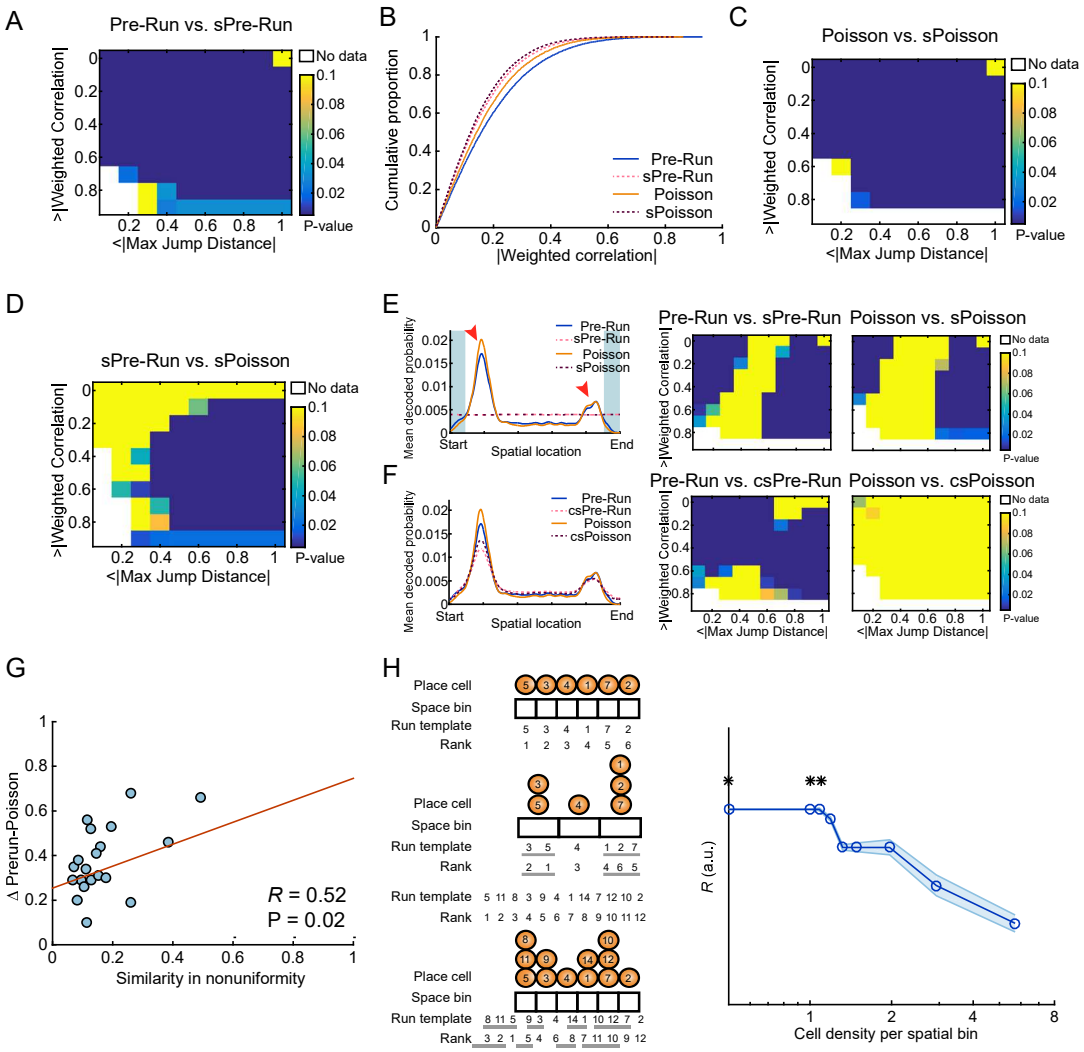

Figure S3. Related to Figures 1, 2 and 4. Robust preplay of future de novo Run trajectory during Pre-Run sleep with corrected space-bin shuffle.
(A) Two-feature P-value matrices testing significance of: preplay versus its space-bin shuffle sPre-Run. This comparison reveals higher trajectory sequential content in preplay compared to its respective sPre-Run.
(B) Comparison of weighted correlations of all Pre-Run sleep, sPre-Run, rate-matched Poisson surrogates, and sPoisson frames. Trajectory sequential content in Pre-Run sleep significantly exceeds that of sPre-Run, Poisson surrogates and sPoisson frames (Pre-Run sleep mean: $0.1916\pm7.6\times10^{-4}$ >> Poisson mean: $0.1701\pm6.7\times10^{-4}$ >> sPreRun mean: $0.1540\pm6.2\times10^{-4}$ >> sPoisson mean: $0.1464\pm5.9\times10^{-4}$; Pre-Run preplay vs. sPre-Run: $P<10^{-10}$; Poisson vs. sPoisson: $P<10^{-10}$; Pre-Run preplay vs. Poisson: $P<10^{-10}$; Pre-Run preplay vs. sPoisson: $P<10^{-10}$; Poisson vs. sPre-Run: $P<10^{-10}$; sPre-Run vs. sPoisson: $P<10^{-10}$, Wilcoxon's ranksum test).
(C-D) Two-feature P-value matrices testing significance of: Poisson data versus its space bin shuffle sPoisson (C) and sPre-Run versus sPoisson (D). Higher sequential structure is observed in Poisson compared to sPoisson, however, the sequential content in sPre-Run exceeds that of sPoisson (indicative of differences between Pre-Run sleep and its Poisson surrogates. These differences appear to have been overlooked in the study of (Silva et al., 2015)).
(E) Discrepancy between non-uniformity in the mean decoded location probabilities in Pre-Run sleep (red arrowheads) and almost perfect uniformity in the corresponding five-hundred sPre-Run (Left, data from one animal). Note that the Poisson data also exhibit similar behavior. The sPre-Run also introduces an edge effect at locations indicated by the black arrows. Preplay versus sPre-Run (Middle) and Poisson versus sPoisson (Right) appear qualitatively similar. These observations led us to hypothesize that the failure to preserve the non-uniformity in the decoded locations in the space-bin shuffles together with the edge effect might have contributed to the reductions in the observed strength of sPoisson datasets (Figure S3C) and the observation of a spurious similarity between the differences between Pre-Run sleep and Poisson surrogates and their respective shuffles.
(F) Compensating for the non-uniformity and the edge effect in sPre-Run and sPoisson (Left, csPre-Run and csPoisson, same Pre-Run and Poisson as in (E)) results in maintenance of significance between Pre-Run and csPre-Run (Middle), but not between Poisson and its csPre-Run (Right).
(G) Degree of similarity between probabilities of decoded location across the track in Pre-Run and in csPre-Run positively correlates with the difference between Pre-Run and Poisson datasets with their respective shuffles (csPre-Run and csPoisson).
(H) Simulation of template matching method showing inability to detect p/replay in a generic sleep session at large densities of place cells per spatial bin of linear track. The increased cells/spatial bin density randomizes rank-ordering of place cells with firing peaks within a spatial bin, which now approaches a random place-cell order similar to shuffled datasets (left). Note that this effect might explain, in part, the lack of detecting sleep preplay by template matching in a recent study (Silva et al., 2015) where we estimated cell density per spatial bin to be 1.58 compared with 0.43 in our data. The same would be true for the detection of sleep replay given similar parameters. The use of a smaller spatial bin size, a down-sampling of cell numbers from the highest-density bins, and the use of cross-correlation between place cell pairs to better estimate their real order in run could all improve the accuracy of template matching results. Our demonstration of trajectory preplay using decoding methods (in the above section), does not immediately assume the existence of preplay at the level of neuronal firing order/sequence (Dragoi and Tonegawa, 2011, 2013a, b). This is because the method of trajectory decoding integrates factors that include neuronal firing rates, neuronal coordination at short timescales, and neuronal firing order/sequence (Figure 2D).

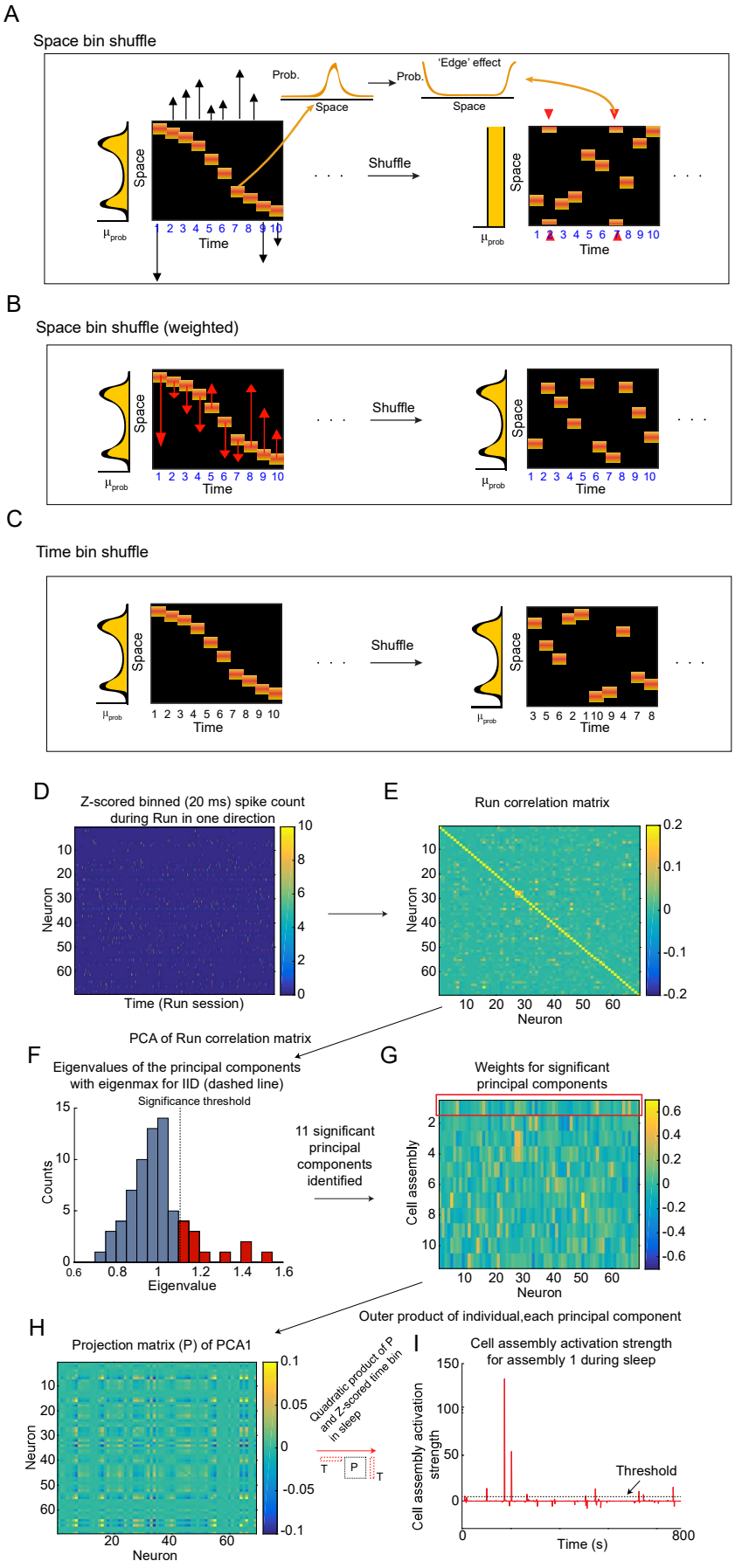

Figure S4. Related to Figures 1 and 5. Schematics depicting shuffles and method for detection and quantification of cell assemblies.

(A-C) Schematic depicting the various shuffles we used and the issues with the use of space bin shuffle.

(A) The circular shift space bin shuffle shifts each spatial bin in a frame independently by a random amount and wraps around the boundaries of the track. Note that this results in some bins having divided maximum decoded locations at the two ends of the track, termed the edge effect, as depicted by the red arrows. Also, the real sleep non-uniformly represents the track, while this shuffle represents the track equally across locations (mean probabilities across the track on left of frame).

(B) Proof-of-concept weighted spatial-bin shuffle designed to support the hypothesis that the results of (Silva et al., 2015) might have been impacted by the use of space-bin shuffle., Peak decoded location was identified in each bin, the average decoded probabilities across bins for the whole sleep were calculated, and the peak decoded location was shifted to a location weighed by that distribution. Note that here, the within-bin spatial structure was conserved as the whole bin was circularly shifted. Furthermore, we did not allow the peak decoded location to be shifted near the edges, reducing division of maxima in decoding.

(C) The time bin shuffle permutes time bins within a frame (depicted by time bin number below the frames). Note that this shuffle overcomes the problems with the space bin shuffle.

(D-I) Schematic representation of the method for detecting cell assemblies (multi-neuronal patterns significantly coactivated during Run). We employed the method developed by (Peyrache et al., 2009) to detect cell assemblies during Run (D). Briefly, neuronal activity for each neuron was binned (20 ms) and Z-scored during Run (independently for each direction) followed by computation of correlation matrix for the Z-scored neuronal activity during the Run (E). Subsequently, a principal component (PC) analysis was performed and significant PCs were identified by computing the eigenvalue for each PC and comparing it to the max eigenvalue expected for IID (F). The weights for each significant PC (G) were used to generate a projection matrix by taking its outer product (H) and setting the diagonal to zero. Following this, a quadratic dot product of this projection matrix, P, with the binned (20 ms) and Z-scored sleep activity, T, was computed to identify peaks in cell assembly activation during the sleep (I). Note that maximum of cell assembly activation (cell assembly activation epoch) occurring within frames was used for further analysis. The threshold for cell-assembly was set at a minimum activation strength of 5 (Peyrache et al., 2009) and a minimum of 2 participating neurons within 20 ms.

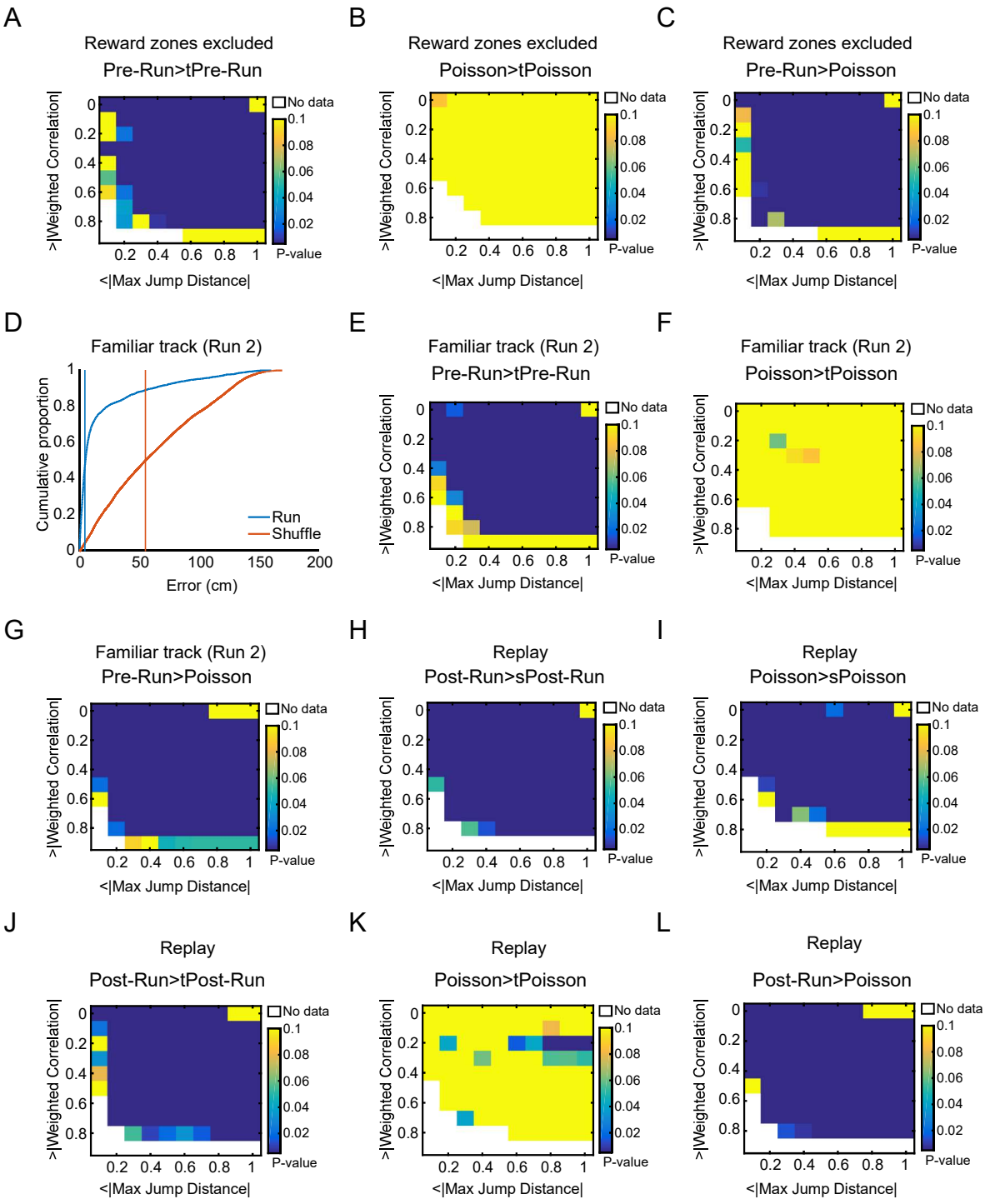

Figure S5. Related to Figure 1. Preplay of de novo Run session with reward locations removed from the analysis, preplay in naive Pre-Run sleep preceding Run 2 on a familiar track and replay of a de novo track.
(A-C) P-value matrices for comparisons of: Pre-Run sleep with its time bin shuffle (A), firing-rate matched Poisson with its time bin shuffle (B) and Pre-Run with its five-hundred Poisson surrogate datasets (C), with reward locations excluded from analysis.
(D) Error in decoded location for a familiar track (Run 2). The error is significantly lower (4.8 cm; Run 2 vs shuffle: Wilcoxon's ranksum test, $P<10^{-10}$) compared with that for the same track during de novo Run (7.6 cm; de novo exposure; Wilcoxon's ranksum test, $P<10^{-10}$). Vertical lines represent medians of corresponding distributions.
(E-G) P-value matrices for comparisons of: Pre-Run with its time bin shuffle (E), firing-rate matched Poisson with its time bin shuffle (F) and Pre-Run with its five-hundred Poisson surrogate datasets (G) for a familiar track.
(H-L) P-value matrices for comparisons of: Post-Run sleep with its space bin shuffle (H), firing-rate matched Poisson with its space bin shuffle (I), Post-Run with its time bin shuffle (J), firing-rate matched Poisson with its time bin shuffle (K) and Post-Run sleep with its five-hundred Poisson surrogate datasets (L). Note that the differences between Pre-Run and Post-Run are not apparent when compared indirectly as in (Silva et al., 2015). We performed a direct comparison in Figure 2C to reveal a significant difference.

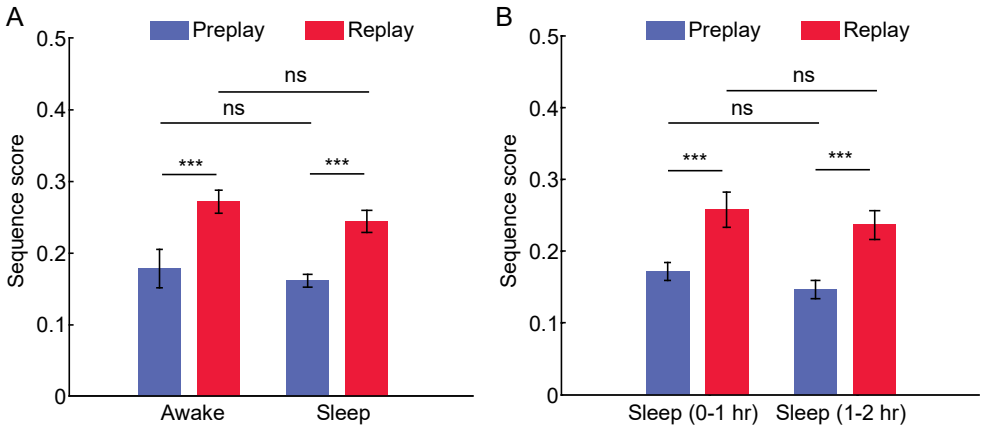

Figure S6. Related to Figures 1, 2, 5 and 6. Dynamics of sequences as a function of duration from experience.
(A) Sequential content increases from preplay to replay even when more stringent criteria for sleep detection are applied. Awake replay in the sleep box is not stronger than sleep replay in the sleep box when these criteria are applied.
(B) Sequential content of trajectory sequences is not a function of duration from experience.

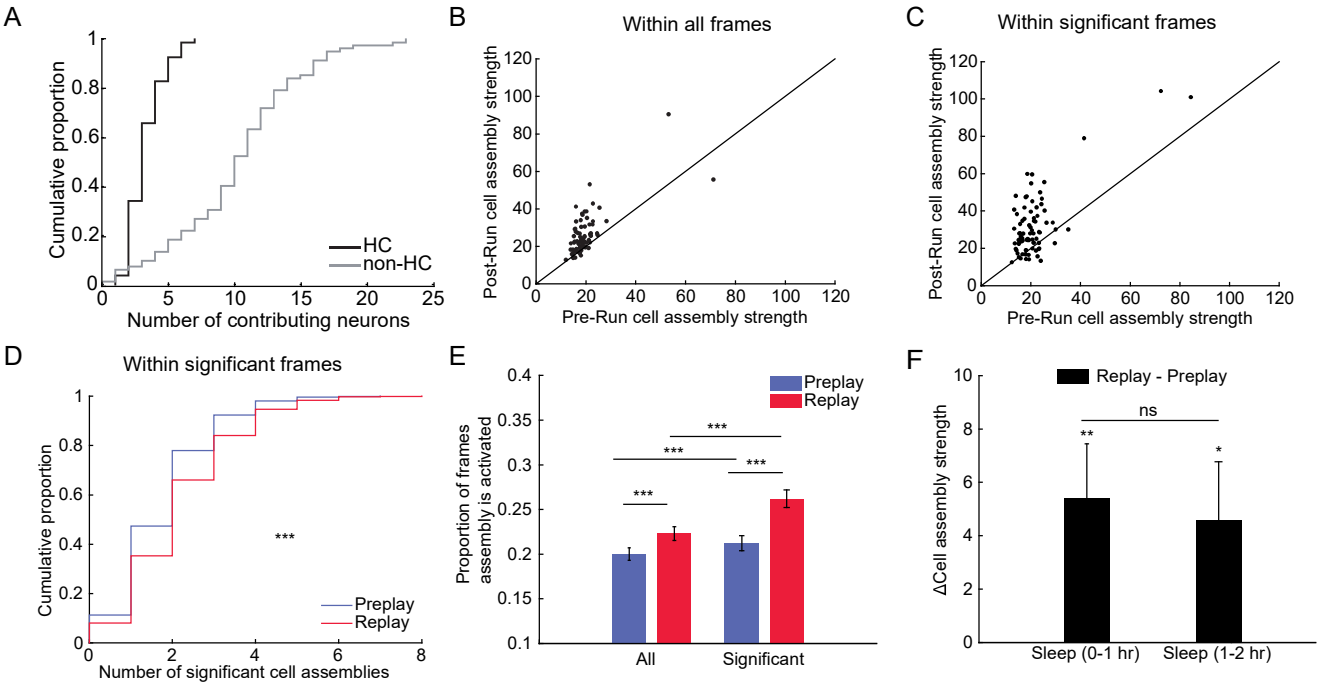

Figure S7. Related to Figures 5. Plasticity of cell assemblies and neurons within cell assemblies.
(A) Number of HC and non-HC neurons per cell assembly.
(B-C) Mean cell assembly strength of individual cell assemblies in the Pre-Run and Post-Run for all frames (B) and for significant frames (C).
(D) Number of significant cell assemblies in significant frames.
(E) Proportion of all and significant frames in which a cell assembly is activated.
(F) Cell assembly strength of trajectory sequences in sleep is not a function of duration from experience. There is a significant and similar increase from preplay to replay in sleep sessions recorded at 0-1 h and 1-2 h from experience.

Table S1. Related to Figures 1-6. Number of place cells, number of significant cell assemblies and decoding error in *de novo* Run session.

Rat ID	#Place cells direction 1	#Place cells direction 2	Median decoding error (cm)	Median decoding error (cm)	# Cell assemblies direction 1	# Cell assemblies direction 2
Rat1	30	31	5.74	7.93	8	8
Rat2	24	25	8.25	9.24	6	6
Rat3	31	37	7.11	7.00	10	9
Rat4	43	45	6.90	8.34	8	11
Rat5	30	28	7.31	8.77	9	7

Table S2. Related to Figures 1-6. Sleep duration and number of frames in Pre-Run and Post-Run sleep sessions.

Rat ID	Pre-Run sleep duration (h)	Post-Run sleep duration (h)	Pre-Run #frames	Post-Run #frames
Rat1	3.05	1.12	4408	830
Rat2	3.31	2.36	2284	1869
Rat3	4.73	2.62	4305	2227
Rat4	4.70	1.90	5248	1591
Rat5	1.53	1.94	2272	2167